Quaternary Science Reviews 303 (2023) 107971

Contents lists available at ScienceDirect

Quaternary Science Reviews

journal homepage: www.elsevier.com/locate/quascirev

Directionally supervised cellular automaton for the initial peopling of sahul

Corey J.A. Bradshaw [a, b, *], Stefani A. Crabtree [b, c, d, e], Devin A. White [d, f, g], Sean Ulm [b, h], Michael I. Bird [b, i], Alan N. Williams [b, j, k], Frédérik Saltré [a, b]

[a] Global Ecology | Partuyarta Ngadluku Wardli Kuu, College of Science and Engineering, Flinders University, GPO Box 2100, Adelaide, South Australia, 5001, Australia
[b] ARC Centre of Excellence for Australian Biodiversity and Heritage. EpicAustralia.org.au, Australia
[c] Department of Environment and Society, Utah State University, 5200 Old Main Hill, Logan, UT, 84322, USA
[d] The Santa Fe Institute, 1399 Hyde Park Road, Santa Fe, NM, 87501, USA
[e] Université de Paris, INSERM U1284, Centre for Research and Interdisciplinarity (CRI), F-75006, Paris, France
[f] Autonomous Sensing and Perception, Sandia National Laboratories, Albuquerque, NM, 87123, USA
[g] Department of Anthropology, University of Tennessee, Knoxville, 502 Strong Hall, Knoxville, TN, 37996, USA
[h] College of Arts, Society and Education, James Cook University, PO Box 6811, Cairns, Queensland, 4870, Australia
[i] College of Science and Engineering, James Cook University, PO Box 6811, Cairns, Queensland, 4870, Australia
[j] Climate Change Research Centre, School of Biological, Earth and Environmental Sciences, University of New South Wales, 2052, Australia
[k] EMM Consulting Pty Ltd, Suite 01, 20 Chandos Street, St Leonards, New South Wales, 2065, Australia

ARTICLE INFO

Article history:
Received 6 October 2022
Received in revised form
18 January 2023
Accepted 19 January 2023
Available online xxx

Handling Editor: Donatella Magri

Keywords:
Superhighways
Human ecology
Archaeology
Population expansion

ABSTRACT

Reconstructing the patterns of *Homo sapiens* expansion out of Africa and across the globe has been advanced using demographic and travel-cost models. However, modelled routes are *ipso facto* influenced by migration rates, and *vice versa*. We combined movement 'superhighways' with a demographic cellular automaton to predict one of the world's earliest peopling events — Sahul between 75000 and 50000 years ago. Novel outcomes from the superhighways-weighted model include (*i*) an approximate doubling of the predicted time to continental saturation (~10,000 years) compared to that based on the directionally unsupervised model (~5000 years), suggesting that rates of migration need to account for topographical constraints in addition to rate of saturation; (*ii*) a previously undetected movement corridor south through the centre of Sahul early in the expansion wave based on the scenarios assuming two dominant entry points into Sahul; and (*iii*) a better fit to the spatially de-biased, Signor-Lipps-corrected layer of initial arrival inferred from dated archaeological material. Our combined model infrastructure provides a data-driven means to examine how people initially moved through, settled, and abandoned different regions of the globe.

1. Introduction

Our knowledge of the patterns and timing of initial peopling of entire continents following the expansion of modern *Homo sapiens* out of Africa has advanced considerably in recent years. Foundational studies have used agent-based models and cellular automata to take into account population saturation, expansion, and demographic structure (Romanowska et al., 2017; Young and Bettinger, 1995) to examine the speed at which populations expand. Other studies have examined how the costs of travel could have constrained populations and led to the characteristic patterns of material culture detected today (Frachetti et al., 2017). Yet, the routes that we can detect would have been influenced by the rates of expansion, and *vice versa*. Examining these two intertwined phenomena in combination is therefore important for reconstructing the history of our species and for exposing how and why human populations developed.

One of the oldest peopling events for which archaeological and genetic data have been sufficient to construct dynamic models of movement and likely spatial use occurred through Sahul — the combined landmass of New Guinea, mainland Australia, and

* Corresponding author. Global Ecology | Partuyarta Ngadluku Wardli Kuu, College of Science and Engineering, Flinders University, GPO Box 2100, Adelaide, South Australia, 5001, Australia.
E-mail address: corey.bradshaw@flinders.edu.au (C.J.A. Bradshaw).

https://doi.org/10.1016/j.quascirev.2023.107971

Tasmania that existed during most of the Late Pleistocene. Data and models suggest that the initial entries of large (Bradshaw et al., 2019), well-organised (Bird et al., 2019) groups of people arriving from Wallacea into Sahul occurred sometime between 75 and 55 ka (1 ka = 1000 years ago) (Bradshaw et al., 2021; Clarkson et al., 2017). The likely major routes of entry are still debated (Bird et al., 2018, 2019; Kealy et al., 2018; Norman et al., 2018; Yuen et al., 2019), but various types of computational modelling (Bradshaw et al., 2021) and genetic data (Bergström et al., 2016; Malaspinas et al., 2016; Nagle et al., 2017; Pedro et al., 2020; Roberts-Thomson et al., 1996; Tobler et al., 2017) support multiple (Bird et al., 2018, 2019; Nagle et al., 2017; Norman et al., 2018; Pedro et al., 2020; Yuen et al., 2019) entry points, most likely using watercraft (Bird et al., 2019; Bradshaw et al., 2021), via a dominant southern route through Bali and Timor into the modern-day Kimberley region of Western Australia, and a secondary northern route into New Guinea through Sulawesi, with the former likely occurring before the latter (Bradshaw et al., 2021).

With the advent of more efficient computational modelling and sophisticated genetic approaches, some questions of the spread into Sahul have been addressed. For example, Norman et al. (2018) suggested multiple probable entry points from Wallacea by leveraging agent-based modelling and network analysis. Esmée Webb and Rindos (1997) also applied models that took into account ^{14}C dates to connect different points across Sahul (and the Americas) probabilistically, suggesting a mode and tempo of peopling. While the collation of information from human mitochondrial genomes has suggested limited dispersal across Sahul (Pedro et al., 2020) and small initial founding populations (Allen and O'Connell, 2020; Bulbeck, 2007), later models contest the idea of small founding populations (Bradshaw et al., 2019). Information from human viruses (Yuen et al., 2019) also suggests an old founding event with spread throughout Sahul. These studies all converge on early arrival dates, and indicate mechanisms of spread, but did not connect the routes of movement or the rates of spread.

Two sister papers (Bradshaw et al., 2021; Crabtree et al., 2021) published simultaneously in 2021 modelled different components of the likely patterns and rates of initial human expansion throughout Sahul. Crabtree et al. (2021) created a fine-scale layer of most-likely movement routes throughout Sahul based on a high-resolution digital elevation model, a fine-scale viewshed of landscape prominence, and least-cost models of pedestrian movement. Based on over 125 billion potential pathways across the continent, the routes best matching the oldest available archaeological evidence had the highest probabilities of travel, to which the term 'superhighways' was applied (Crabtree et al., 2021). Bradshaw et al. (2021) developed a stochastic-ecological, cellular-automaton model where population growth and movement were functions of climate-hindcasted inferences of human carrying capacity, water availability, landscape ruggedness, and stochastic disturbance events. Compared to the oldest available archaeological data, the patterns of expansion and settlement arising from scenarios where different variants of timing and point(s) of entry, as well as the assumed form of the relationship between landscape productivity and human carrying capacity, indicated continental saturation was possible within 4368–5599 years (or, 156–208 human generations) from initial entry (Bradshaw et al., 2021) — a rate of 0.78–0.92 km year^{-1}.

While the different aims and approaches of the two papers both considered elements of human movement patterns, neither directly incorporated inferences from the other. It is therefore timely to combine the two approaches into a single modelling framework to fine-tune inferences of both the spatial pattern and rates of initial peopling of Sahul. The addition of the superhighways probability layer directly accounts for finer-scale subtleties of terrain effects on human endurance and physiology, as well as a more mechanistic link to available water — elements missing or simplified in the directionally unsupervised cellular-automaton model.

Here we describe in detail how we modified the cellular-automaton model (Bradshaw et al., 2021) by formally incorporating the pathway probabilities predicted from the superhighways model (Crabtree et al., 2021) to include both routes and rates of expansion, and test the following two hypotheses: (*i*) Cell-based movements of human populations weighted by the terrain features best-suited to human migration should slow the progression of continental saturation predicted from the initial model. We predict a slower progression because weighting will reduce the frequency of shortest-path routes toward destination cells. (*ii*) The amalgamation of the two models will shift the patterns of initial arrival predicted by the unsupervised cellular automaton toward the superhighways.

The combined model provides a more data-driven means to examine how people might have moved through, settled, and abandoned regions of the continent after the initial period of peopling, especially during future periods of climatic stress as is thought to have occurred during the Last Glacial Maximum (29 ka–18 ka) (Cadd et al., 2021) in many of the more arid parts of Sahul (Williams, 2013; Williams et al., 2013). Further, this approach demonstrates how combining sophisticated continental-scale path modelling with data-driven cellular automata or agent-based models can shed light on the complicated process of peopling a continent. Together these models allow for a better framework and understanding of the archaeological and genetic data currently available in Sahul, and reveal a promising avenue for future research into other past peopling events in other continents.

2. Methods

While the detailed methods for the derivation of the superhighways layer and the cellular automaton are described in detail in the original articles (Bradshaw et al., 2021; Crabtree et al., 2021), we briefly summarise both approaches, and then explain how we combined the two.

2.1. Superhighways model

Described in Crabtree et al. (2021), we created a 500 m-resolution digital elevation model that linked modern New Guinea, Australia, and Tasmania into one supercontinent (Sahul), including now-submerged areas. We then built two additional spatial layers that calculated (*i*) the visibility of all landforms across Sahul based on the topography from the digital elevation model, and (*ii*) the most probable permanent bodies of water based on streams of Strahler Order 9, and extended to the ancient coastline. These three layers provided the base landscape information needed for the traveller model.

To model human travellers, we simulated scenarios of travel across Sahul using the From Everywhere To Everywhere modelling platform (White and Barber, 2012). Unlike standard least-cost path analyses, From Everywhere To Everywhere examines the costs of travelling across every cell on the landscape, assuming that people would use other decisions aside from minimizing travel costs when transecting a landscape. By combining four well-known travel-cost functions, we created a cost surface against which we could examine multiple travel scenarios. First, Tobler's hiking function (Tobler, 1993) estimated walking speed as a function of slope. That speed estimate was then supplied, along with an estimate of terrain roughness, traveller weight, and additional load carried to either Pandolf's equation (Pandolf et al., 1977) for flat or uphill travel or

Santee's equation (Santee et al., 2003) for downhill travel. The end result was an estimate of metabolic rate compared to a standing rate estimated from the Mifflin St. Jeor equation (Frankenfield et al., 2005; Mifflin et al., 1990) (inputs are traveller age, height, and gender), the larger of which was used to calculate energy burned by the traveller as a function of walking speed and distance. We then modelled several scenarios of continent exploration, including: travellers moving from the coasts to other coasts, travellers moving toward fresh water, and travellers using high points on the landscape for wayfinding, weighting the associated costs for the latter two scenarios by traveller proximity to water bodies and prominent landforms, respectively (closer proximity resulting in lower costs). As travellers moved from their origin point to their input destination points for these various scenarios, we simulated over 125 billion possible pathways. We estimated pixel attractiveness as the number of times it is crossed in the movement simulations with the pixels that were traversed more frequently deemed as more attractive. We then subset the 125 billion pathways to the top 1%, 5%, or 10% most frequently chosen paths.

To determine how these possible pathways corresponded to probable migration routes, we developed statistical methods (including a modification of Ripley's *K*-function (Kiskowski et al., 2009) that enabled the comparison of point to network data), to compare networks of potential pathways against archaeological data (sites of ≥30000 years old). These archaeological data are provided in the Supplementary of Crabtree et al. (2021) (also see 'Data availability' statement below). In brief, the dataset consisted of 560 radiocarbon dates distributed across Sahul, including New Guinea and Australia, with each assigned a ranking based on the relevant dating methodology and association with archaeological materials. Here, the spatial distribution of the oldest archaeological sites was used to determine the best-supported pathways, because there was no temporal component in the model. Specifically, we treated a network of paths as a single spatial feature against which we compared the distribution of archaeological sites. When the archaeological sites corresponded more closely with a path on a given network, the path was given stronger probabilistic weight for explaining the network. In this way, we could examine which of the most frequently chosen paths most closely corresponded to real archaeological data, and then combine them using an approach based on the Bayesian information criterion to produce a composite network of most likely chosen routes across the continent that reflected multiple traveller motivations.

2.2. Cellular automaton

Described in Bradshaw et al. (2021), we constructed a raster model based on a 0.5° × 0.5° latitude/longitude grid of Sahul, estimating exposed land in 1000-year time slices to follow available hindcasts of carrying capacity. From an initially peopled cell, the new population grew following a Ricker population-dynamics model that estimated the change in human abundance (N) as:

$$N_{i,j,t+1} = N_{i,j,t} e^{r_m\left(1-\frac{N_{i,j,t}}{K_{i,j,t}}\right)} - \left(E_{i,j,t} - I_{i,j,t}\right) \quad [1]$$

where i is the cell row number in the 0.5° × 0.5° latitude grid, j is the cell column number, t is the time interval in units of human generations (1 generation = 27.9 years) (Bradshaw et al., 2019), $N_{i,j,t+1}$ is the number of individuals in cell i, j at the next time interval $(t + 1)$, $N_{i,j,t}$ is the number of individuals in cell i, j at time interval t, r_m is the maximum rate of population increase when resources are not limiting, $K_{i,j,t}$ is the cell-specific carrying capacity, and the $E_{i,j,t}$ and $I_{i,j,t}$ represent the number of individuals emigrating from and immigrating into the focal cell i, j per time interval t, respectively (Fig. 1).

We derived theoretical carrying capacity (K) for each cell from a hindcasted estimate of net primary production based on the LOVECLIM climate reconstruction (Bird et al., 2019; Bradshaw et al., 2019; Goosse et al., 2010). LOVECLIM is a three-dimensional Earth-system model (Goosse et al., 2010) that produces climates over the past 800 ka in 1000-year time-averaged increments (layers) that we downscaled (using a bilinear interpolation) (Lorenz et al., 2016; Wilby and Wigley, 1997) from a spatial resolution of 5.625° × 5.625°–0.5° × 0.5°. For each grid cell and each 1000-year layer, net primary production (Timmermann and Friedrich, 2016) (kg C m^{-2} $year^{-1}$) was the indicator of relative carrying capacity through time (Bradshaw et al., 2019), translated into human carrying capacity (Tallavaara et al., 2018) following evidence for nonlinearity (Bradshaw et al., 2019) — a 180°-rotated parabola function between K and net primary production (P_p):

$$K = a\left(P_p - h\right)^2 + K_{\max} \quad [2]$$

where $K_{\max} = 0.5K_{\max}$ from a linear relationship, $a = -3$, h = the median of P_p.

Emigration out of a focal cell i,j to its eight immediate neighbours was a function of the gradient in K_t between two cells (Vahdati et al., 2019) (Fig. 1b), as well as how close the abundance $N_{i,j,t}$ of cell i, j was to $K_{i,j,t}$. An exponential decay function to describe the declining probability of emigration (Pr(E)) as the ratio of $K_{i,j,t}/K_{i+y,j+x,t} = K_{\text{rel}}$ increased toward 1 was imposed, where:

$$\Pr(E) = e^{-3.2K_{\text{rel}}}$$

The size of the emigrating group N_{mig} was a beta-resampled proportion $P_{\text{mig}} = 1/3$, such that N_{mig} was centred on $N_{i,j,t} \times P_{\text{mig}}$ (with SD = $0.05N_{i,j,t} \times P_{\text{mig}}$) (McNiven, 1999), and applied for each of the eight cell comparisons. When $K_{i,j,t}/K_{i+y,j+x,t} > 1$, immigration into cell i, j occurred following the same movement rules. We also imposed long-distance dispersal as an estimated probability of dispersing a maximum distance ($d_{\max}$), with corrections for landscape productivity (Hiscock, 2008; O'Connell and Allen, 2012), ruggedness (Binford, 2001), and a distance-to-water limitation (Bird et al., 2016; Saltré et al., 2009) (Fig. 1).

Upon initializing a population-growth and movement iteration (per generation), we imposed a spatially contagious catastrophic mortality function (Chamberlain, 2009) following a Thomas cluster process (Baddeley et al., 2015) (i.e., each cell designated for catastrophic mortality is identified according to two independent, zero-mean normal variables with variance σ^2 describing cell's x and y coordinates relative to the centre of a Poisson cluster). This function emulated random occurrences of a large disturbance generated, for instance, by bushfires, diseases, cyclones, floods, or warfare.

We ran each stochastic set-up of the cellular-automaton model with various starting conditions (entry times and sequences) as well as different assumptions of the relationship between carrying capacity and net primary production, repeating each scenario 100 times to generate a per-cell confidence interval of time of first arrival. Using a similar archaeological dataset as for the super-highways model (see 'Data accessibility' statement), but instead incorporating the full uncertainty in high-reliability estimated radiocarbon dates (for a full description of reliability assessment of available dates, see https://doi.org/10.5281/zenodo.4453767), as well spatially de-biasing their sampling distribution (Bradshaw et al., 2021; Saltré et al., 2019), we determined which combination of conditions had the best match to the spatio-temporal distribution of the oldest archaeological material across both Australia and New Guinea.

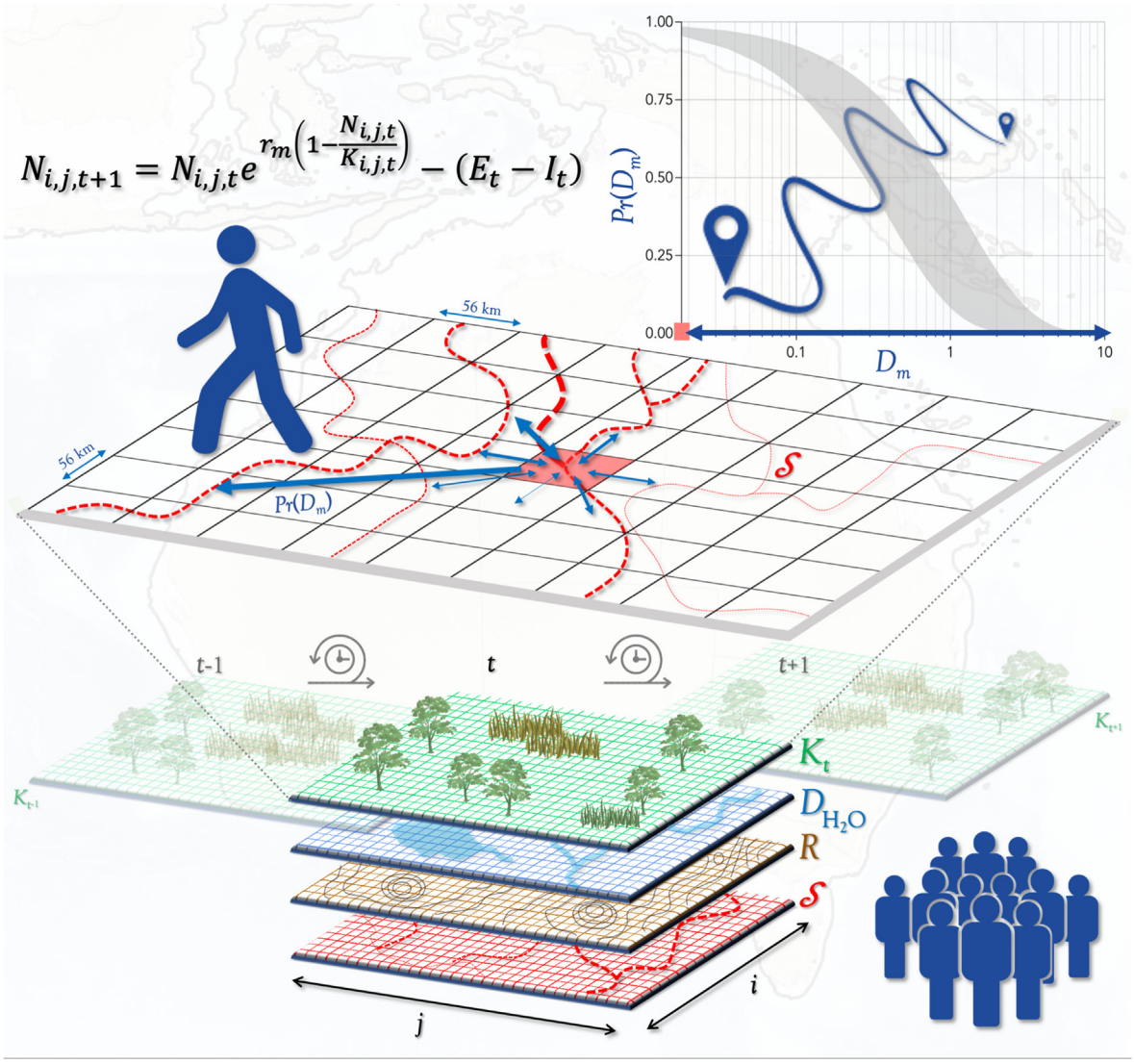

Fig. 1. Schematic of combined model infrastructure and relationship among its major components. (**middle plane**) A single (millennium-scale) 0.5° × 0.5° (~56 km × 56 km) grid (*i* rows and *j* columns) of carrying capacity (K = green layer, lower panel) is calculated from hindcasted net primary production following a 180°-rotated parabola function. Moore neighbourhood emigration/immigration (double-headed dark blue arrows) is a function of the relative carrying capacity (K = green layer, lower panel) between adjacent cells and the superhighways layer ($\mathcal{S}$ = dashed lines in middle plane and red layer in lower layer stack). (**upper right graph**) long-distance dispersal probability $\Pr(D_m)$ (also conditional on $\mathcal{S}$) follows a log-sigmoidal relationship of the form $\Pr(D_m) = e^{-d/aM^b}$, where D_m = distance D exceeding multiples (1–10) of one cell width (0.5 × 111.12 = 55.6 km). Movement of people across the grid is a function of K as described above, but also on distance to water (D_{H_2O} = blue layer, lower layer stack) cell 'ruggedness' (R = brown layer, lower layer stack), and superhighways ($\mathcal{S}$ = red layer, lower layer stack), where backward and adjacent movements (both within the Moore neighbourhood and for long-distance dispersal) are probability-weighted random directions toward a destination cell following rules where forward movements are permitted and backward movements are prohibited. (**equation**) Intrinsic population growth or decline in abundance (N) from time t to t+1 follows a Ricker-logistic function, where r_m = maximum rate of population growth, and E_t and I_t are net emigration and immigration values described above. Variation in millennium-scale time t carrying capacity K is represented by semi-transparent K layers adjacent to the lower layer stack.

2.3. Combined superhighways–cellular-automaton model

Using a range of the best-supported initial conditions from the unsupervised cellular automaton (Bradshaw et al., 2021) (entry time of 75 ka or 50 ka; sequence: southern entry followed by northern entry; and a parabolic relationship between human carrying capacity and net primary production), we weighted the underlying dispersal functions in the cellular-automaton model following the superhighways probability layer (Fig. 1). We first weighted immigration and emigration to and from a focal cell *i*, *j* using a random binomial resample of each of the eight neighbouring cells' superhighway probability $\mathcal{S}$, but standardised for the immediate eight-cell (Moore) neighbourhood such that

$$\mathcal{S}'_{i+\partial i,j+\partial j} = \frac{\mathcal{S}_{i,j}/\mathcal{S}_{i+\partial i,j+\partial j}}{\max_{\exists \mathcal{S}}\left(\mathcal{S}_{i,j}/\mathcal{S}_{i+\partial i,j+\partial j}\right)}$$

where ∂i and ∂j are the relative directions north-south and east-west, respectively (−1 to 1).

Weighting the long-distance dispersal by $\mathcal{S}$ was more complex because of the various multi-cell pathways possible from a focal cell *i*, *j* to the set of possible destination cells derived from the stochastic calculations of d_{max}. Once a destination cell was determined randomly, the path from the focal cell to that destination cell followed a correlative random-walk process with a directional limitation at each cell along the pathway based on $\mathcal{S}$ (i.e., backwards

movements were prohibited as the pathway is built). To progress from cell *i*, *j* to an adjacent cell, we subsequently weighted the randomly chosen direction by $\mathscr{S}$ in the Moore neighbourhood. The adjacent target cell then became the new focal cell, and the directional selection process repeats, only this time backwards movements (to the previously occupied cell and its neighbours) were not allowed (i.e., regressive movements toward the source cell prohibited). We repeated all scenario configurations 100 times each to build mean arrival-time isohyets across the entire continent.

3. Results

As part of an earlier interrogation of the initial peopling of Sahul (Bradshaw et al., 2021), we explored the most probable timeframes for a successful non-extinction peopling. While the exact timing of this initial seeding is not critical to our analysis here, the two timeframes nonetheless encompass the full period currently under debate for people's first arrival in Sahul. Specifically, we adopted the top-ranked scenarios from Bradshaw et al. (2021) consisting of an initial southern entry at 75 ka followed by northern entry at 73 ka, and a single southern entry at 50 ka. When applying these and weighting both the neighbouring-cell immigrations and emigrations, as well as long-distance dispersal, by the superhighways probability layer from Crabtree et al. (2021), the time to continental saturation (i.e., all cells occupied) from initial entry ranged from 7784 to 9347 years (279–335 human generations) for the 75–73 ka double-entry scenario (Figs. 2–4), to 8733–11551 years (331–414 human generations) for the single-entry scenario (Figs. 2, 3 and 5). Contrasting scenarios assesses relative changes in the landscape's potential to support human populations over space and time, and so we express times of initial arrival relative to the assumed date of entry to Sahul instead of fixed dates.

Considering additional scenarios where we altered the timing of initial entry (double or single) showed remarkably similar results, with saturation times varying from 7784 to 11383 years (double entry) to 8593–12667 years (single entry) (Fig. 6). However, there were notable differences in the spatial pattern of movement depending on whether we applied a double or single entry. Without exception, the double-entry scenarios led to a rapid movement along the approximate central meridian of the continent (~131° longitude) toward the Great Australian Bight by ~ 4000 years after initial entry (Figs. 2–4, 6). In contrast, the single-entry scenarios predicted a more gradual expansion toward the south-east of the continent, with arrival in the Great Australian Bight

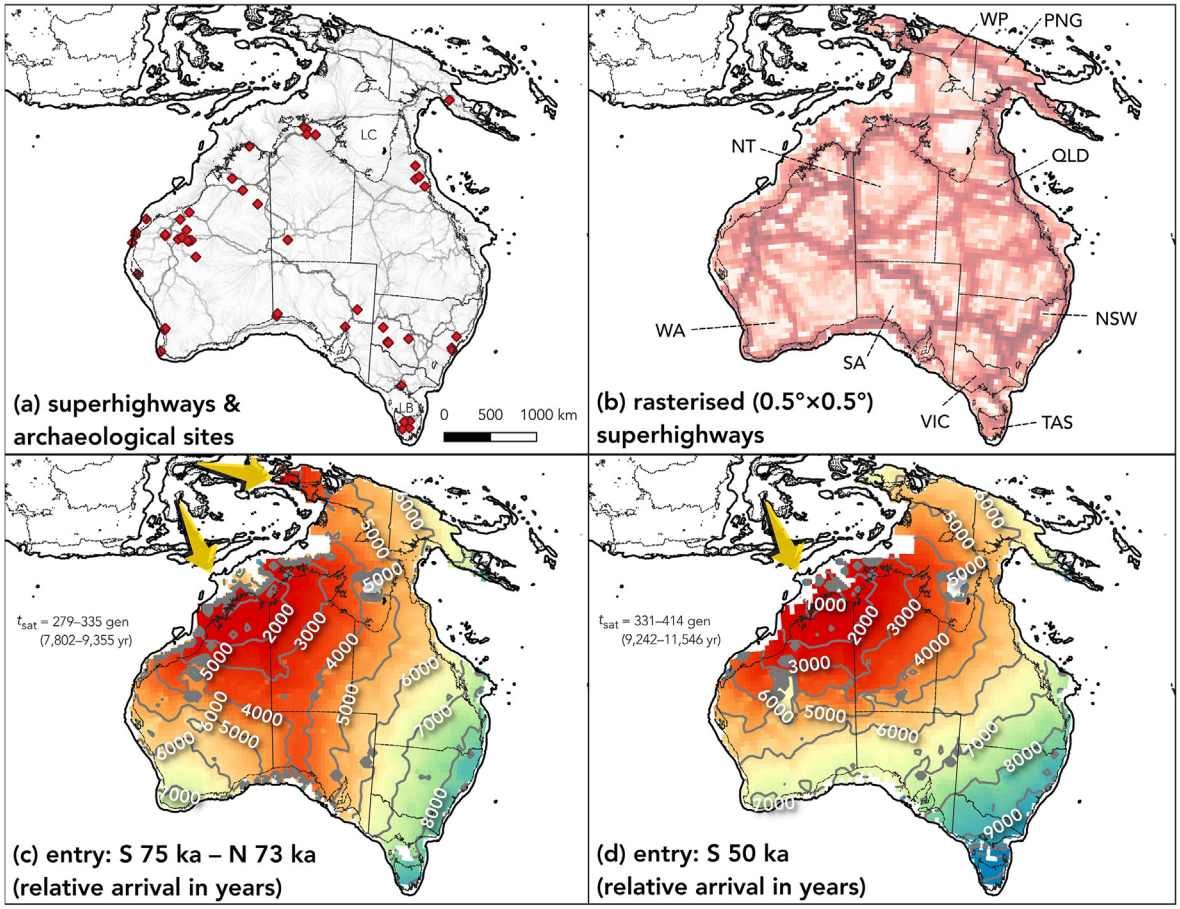

Fig. 2. Main combined model inputs and outputs. (**a**) Fine-scale (10 km) resolution of the dominant movement corridors ('superhighways') derived from Crabtree et al. (2021). LC = Lake Carpentaria; LB = Lake Bass. (**b**) Upscaled (rasterised) version of the superhighways layer to a 0.5° × 0.5° raster grid to match the resolution of the cellular-automaton spread model from Bradshaw et al. (2021). WP = West Papua; PNG = Papua New Guinea; QLD = Queensland; NSW = New South Wales; TAS = Tasmania; VIC = Victoria; SA = South Australia; WA = Western Australia; NT = Northern Territory. (**c**) Combined superhighways-cellular automaton model with an initial entry to Sahul at 75 ka on the now-submerged Sahul Shelf offshore from the modern-day Kimberley region of Western Australia (southern [S] entry; southern amber arrow) followed by a subsequent entry 2000 years later (73 ka) at western Bird's Head (Vogelkopf Peninsula) in modern-day West Papua (northern [N] entry; northern amber arrow). Shown are the 1000-year isohyets of relative initial arrival across Sahul on a colour scale from red (earlier) to blue (later) relative to the timing of initial entry, as well as the time to saturation (t_{sat}; occupation of every cell in Sahul) in both human generations (gen) and years (yr) relative to initial entry (see Fig. 4 for finer-scale details by region). (**d**) As in (c), but with a single initial southern entry at 50 ka (see Fig. 6 for finer-scale details by region).

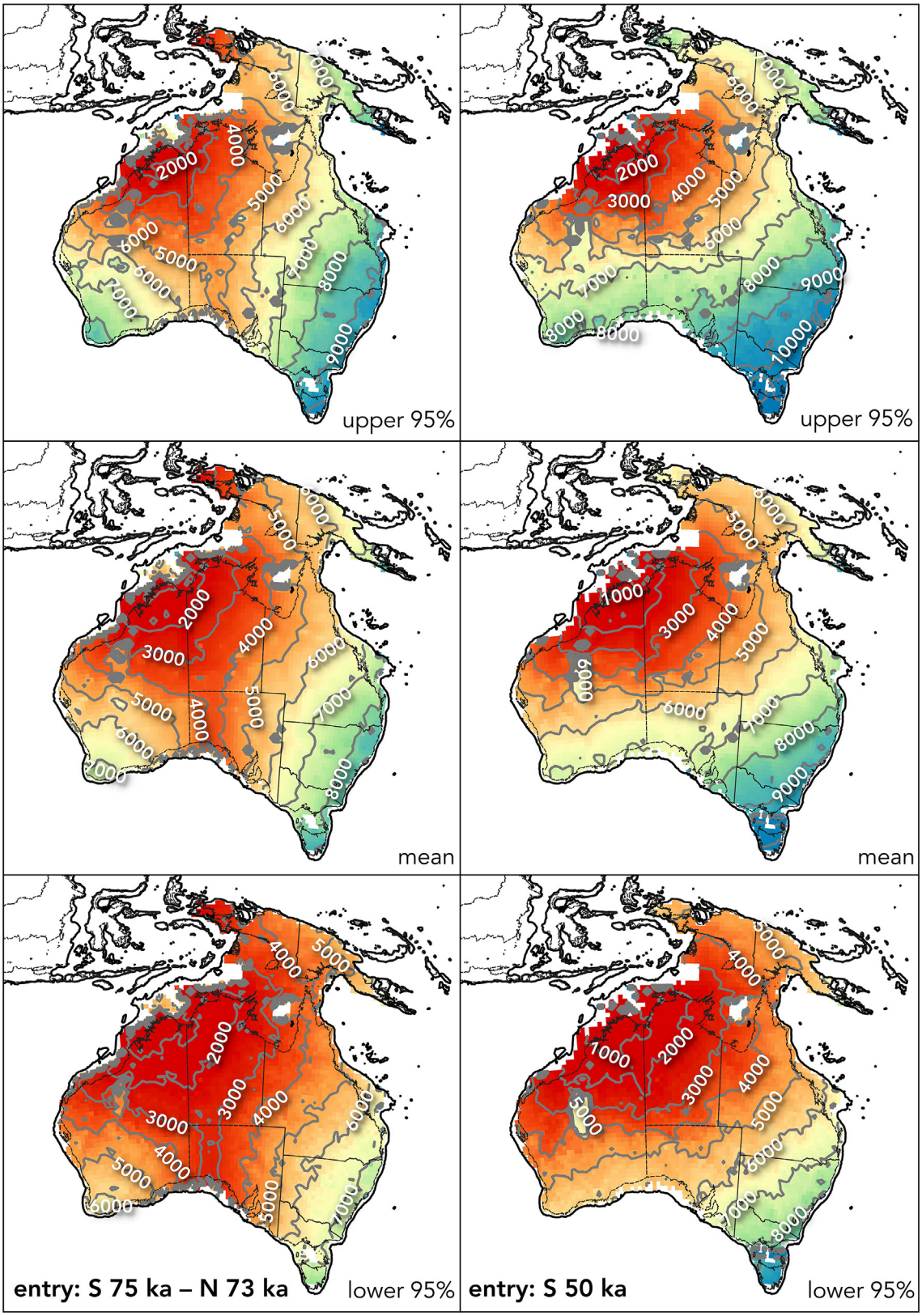

Fig. 3. Upper and lower 95% confidence limits for relative initial arrival time. Left panels show the combined superhighways-cellular automaton model initial arrival estimates (**top**: upper 95% confidence limit; **middle**: mean; **lower**: lower 95% confidence limit) for an initial entry to Sahul at 75 ka on the now-submerged Sahul Shelf offshore from the modern-day Kimberley region of Western Australia (southern [S] entry) followed by a subsequent entry 2000 years later (73 ka) at western Bird's Head (Vogelkopf Peninsula) in modern-day West Papua (northern [N] entry). **Right panels** are as for left panels, but with a single initial southern entry at 50 ka. Shown are the 1000-year isohyets of relative initial arrival across Sahul on a colour scale from red (earlier) to blue (later) relative to the timing of initial entry.

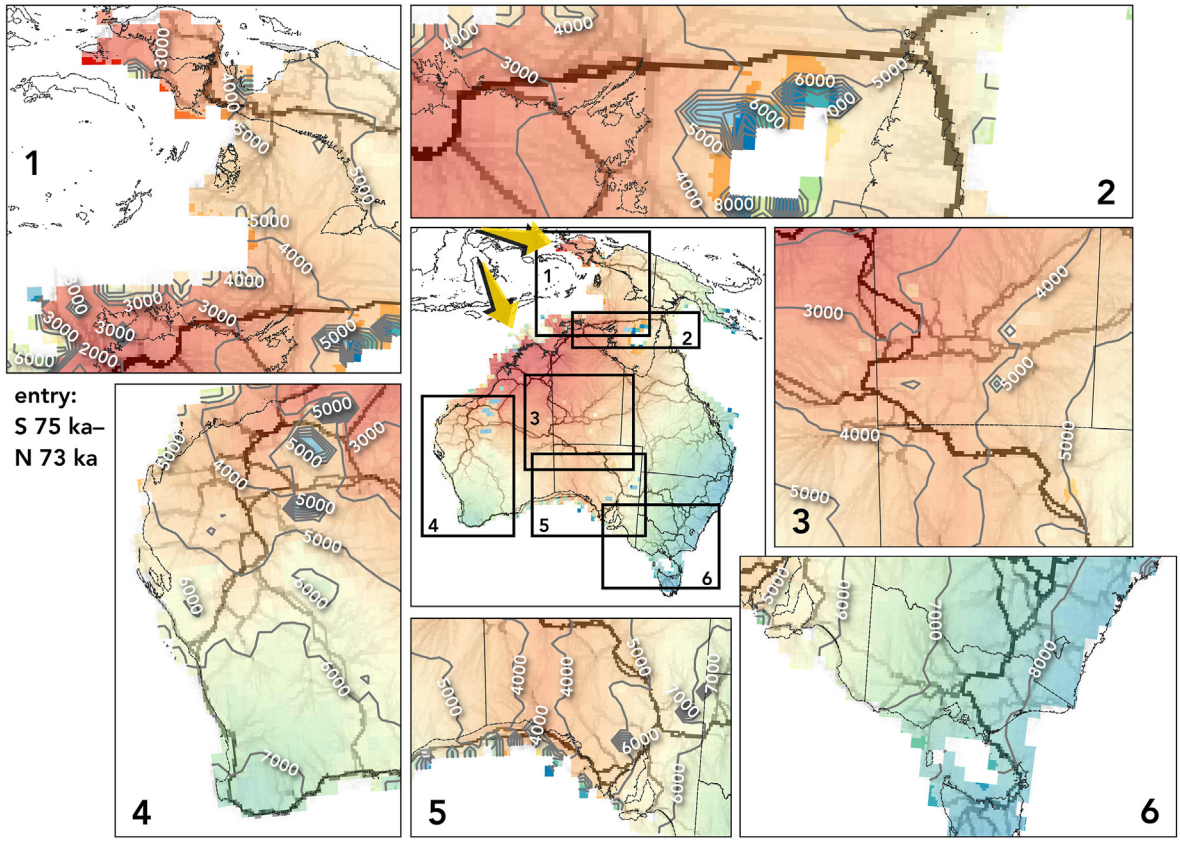

Fig. 4. Mean initial arrival times from the superhighways-supervised cellular automaton (2 entries). Zoomed map insets show finer-scale, regional patterns than the map in Fig. 2c for an initial entry to Sahul at 75 ka. Shown are the 1000-year isohyets of relative initial arrival across Sahul on a colour scale from red (earlier) to blue (later) relative to the timing of initial entry (0.5° × 0.5° resolution), as well as the fine-scale (10 km resolution) superhighways derived from Crabtree et al. (2021). Regionally zoomed boxes cover: (**1**) Arnhem-West Papua, (**2**) Arnhem-Carpentaria, (**3**) central, (**4**) west, (**5**) south central, and (**6**) south east.

occurring almost 4000 years later (at ~ 8000 years after initial arrival) (Figs. 2, 3, 5 and 6). Regardless of the entry scenario, New Guinea was peopled gradually over 5000–6000 years, with a focus initially on the Central Highlands and Arafura Sill before reaching the Bismarck Archipelago. In both cases, however, the peopling of the far southeast and Tasmania is predicted to have occurred between 9000 and 10000 years following initial arrival (Figs. 2, 3, 5 and 6).

Compared to the directionally unsupervised model from Bradshaw et al. (2021) that predicted continental saturation at 4368–5599 years (156–208 generations) following initial entry, the superhighways-weighted models here predicted a rate of continental saturation that was 1.78–2.06 times slower (Fig. 7). While comparing the bias-corrected archaeological map of initial arrival described in Bradshaw et al. (2021) to the predicted initial arrival from our supervised model scenarios is not an independent validation *per se* (i.e., the same archaeological data validated the unsupervised cellular automaton, whereas the spatial distribution of archaeological sites provided a measure of model performance in the superhighways layer), the spatial Spearman's rank correlation (ρ) between the archaeological data (bias-corrected, including the 38 highest-reliability [category *A*] age estimates, but excluding the 10 low-reliability [category *C*] age estimates, from the Madjedbebe site in northern Australia; for a full description of the reliability assessment of available dates, see https://doi.org/10.5281/zenodo.4453767) (Bradshaw et al., 2021; Clarkson et al., 2017) was higher for both the double- and single-entry scenarios in the supervised models (0.222 and 0.206, respectively) compared to the unsupervised models (~0.07–0.21) (Bradshaw et al., 2021). These higher mean correlations confirm a better fit of our predicted initial arrival and saturation data to the available archaeological evidence.

There was no obvious spatial clumping of the correlations between the unsupervised and superhighways-supervised predictions of initial arrival for either of the two main scenarios presented in Fig. 2c and d (i.e., 75 ka S–73 ka N or 50 ka S) (Fig. 8a and b), except for the cluster of mainly negative correlations in the south-central region toward the Great Australian Bight for the 75 ka S–73 ka N scenario (Fig. 8a). Nor was there any apparent spatial pattern in the correlation of predicted initial arrival times for the two main scenarios considered in the superhighways-supervised model (Fig. 8c).

4. Discussion

The timing and mechanisms of the initial peopling of Sahul form a cornerstone of Australian archaeological research going back nearly five decades; initially explored in the 1970s, the phenomenon is still vehemently debated (Allen and O'Connell, 2020; Clarkson et al., 2017; Dortch and Malaspinas, 2017; Hiscock, 2017; O'Connell et al., 2018; Veth, 2017; Wood, 2017). Our predictions contribute to this debate by estimating corrected saturation ages to (*i*) hindcast from more robust archaeological data after 50000 years to provide insights on the dynamics of how the initial peopling might have progressed; and (*ii*) to identify the major mechanisms

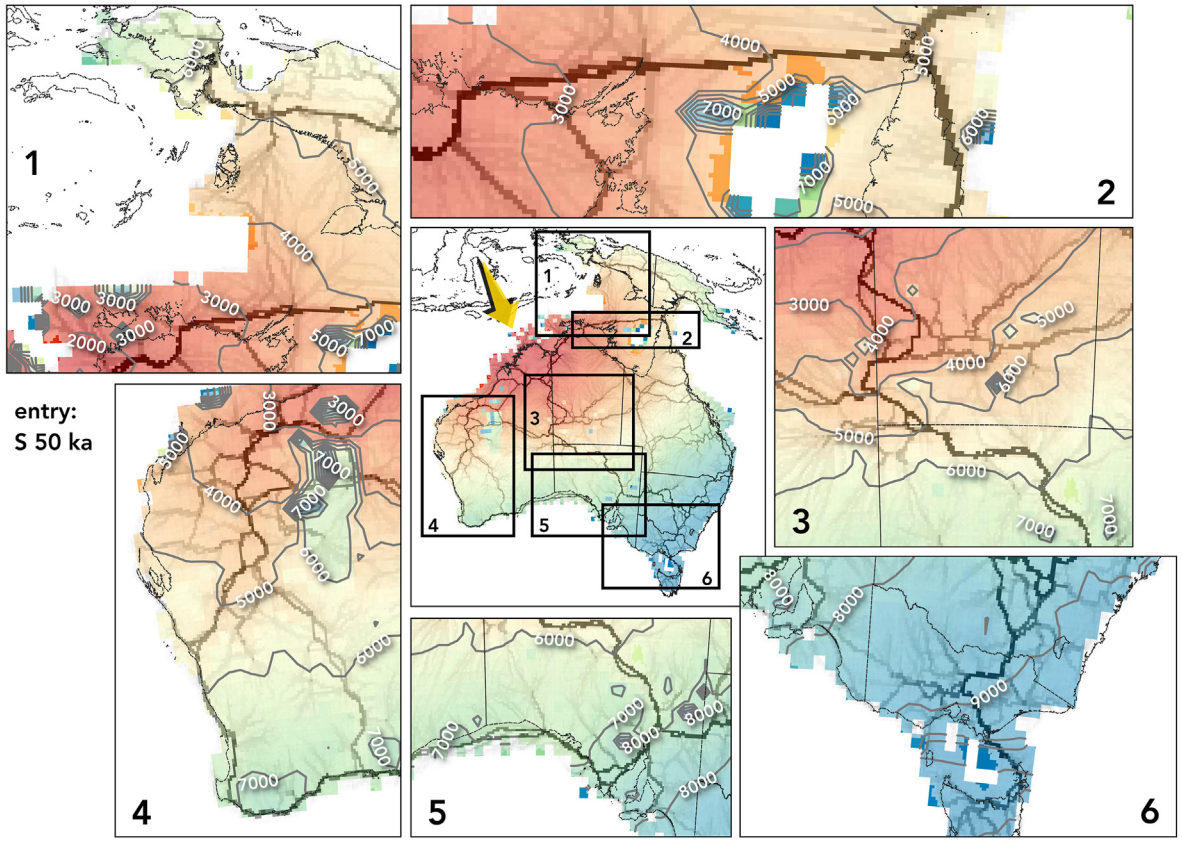

Fig. 5. Mean initial arrival times from the superhighways-supervised cellular automaton (single entry). Zoomed map insets show finer-scale, regional patterns than the map in Fig. 2d for a single, initial entry to Sahul at 50 ka. Shown are the 1000-year isohyets of relative initial arrival across Sahul on a colour scale from red (earlier) to blue (later) relative to the timing of initial entry (0.5° × 0.5° resolution), as well as the fine-scale (10 km resolution) superhighways derived from Crabtree et al. (2021). Regionally zoomed boxes cover: (**1**) Arnhem-West Papua, (**2**) Arnhem-Carpentaria, (**3**) central, (**4**) west, (**5**) south central, and (**6**) south east.

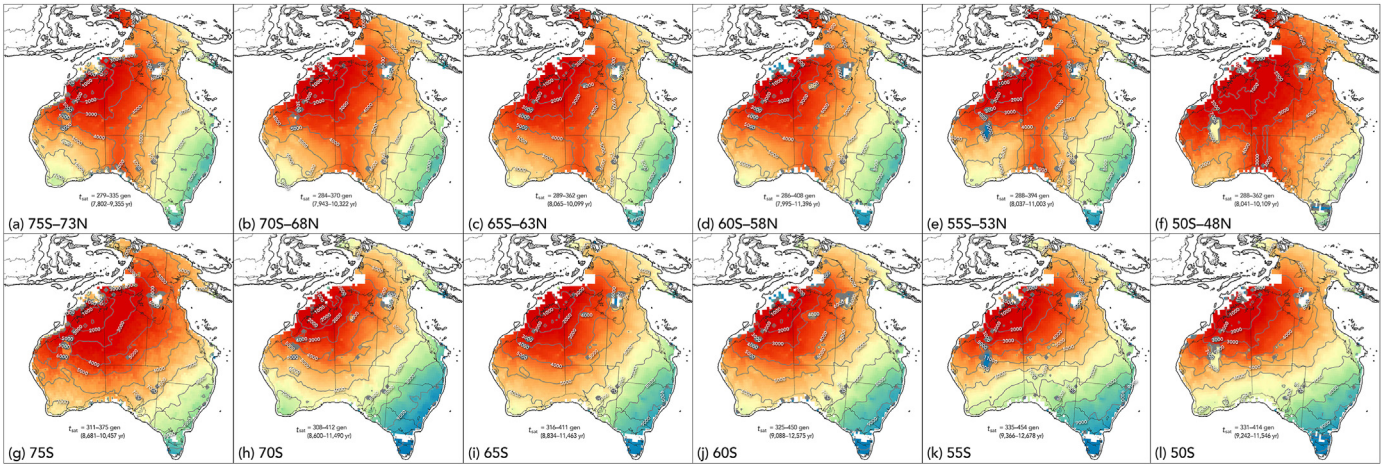

Fig. 6. Patterns of initial arrival varying with timing and pattern of initial entry. Different combinations of entry time in 5000-year increments (50 ka–75 ka) and site of entry (south [S], or [N], or both [S–N], but with the southern entry always occurring first (Bradshaw et al., 2021). Shown are the 1000-year isohyets of relative initial arrival across Sahul on a colour scale from red (earlier) to blue (later) relative to the timing of initial entry, as well as the time to saturation (t_{sat}; occupation of every cell in Sahul) in both human generations (gen) and years (yr) relative to initial entry.

involved in sporadic abandonment and repopulation through later periods of climatic extremes such as the during the Last Glacial Maximum (Williams et al., 2013).

As predicted, the combination of movement functions directionally weighted by the likelihood of human travel as expressed by the superhighways (Crabtree et al., 2021) approximately doubled the simulated time to continental saturation. This is a logical outcome of the fine-scale landscape features and limitations placed on human travellers to choose movement pathways that are not necessarily the shortest distance between two locales (Fig. 7). Of particular interest was the emergence of a dominant movement corridor developing south from the north-western Sahul Shelf

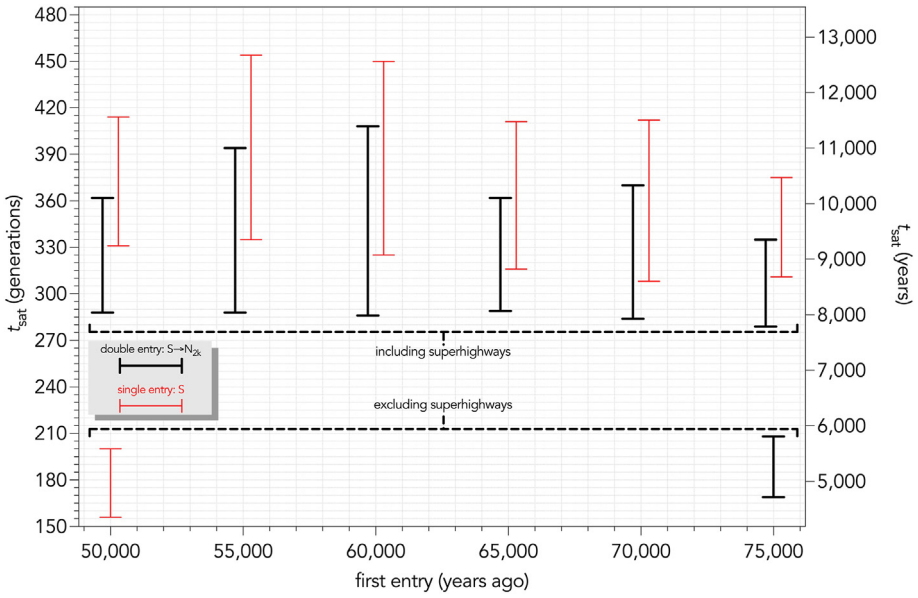

Fig. 7. Time to saturation (t_{sat}; occupation of every cell in Sahul) for both single- (red) and double-entry (black) scenarios measured in both human generations and years relative to initial entry. In all cases, the southern (S) entry precedes the northern (N) entry by 2000 years (2 k). The top ranges combine the superhighways layer with the cellular-automaton model, whereas the bottom two ranges show the most highly supported entry types from Bradshaw et al. (2021). In other words, incorporating the superhighways layer approximately doubled the estimated time to saturation of Sahul.

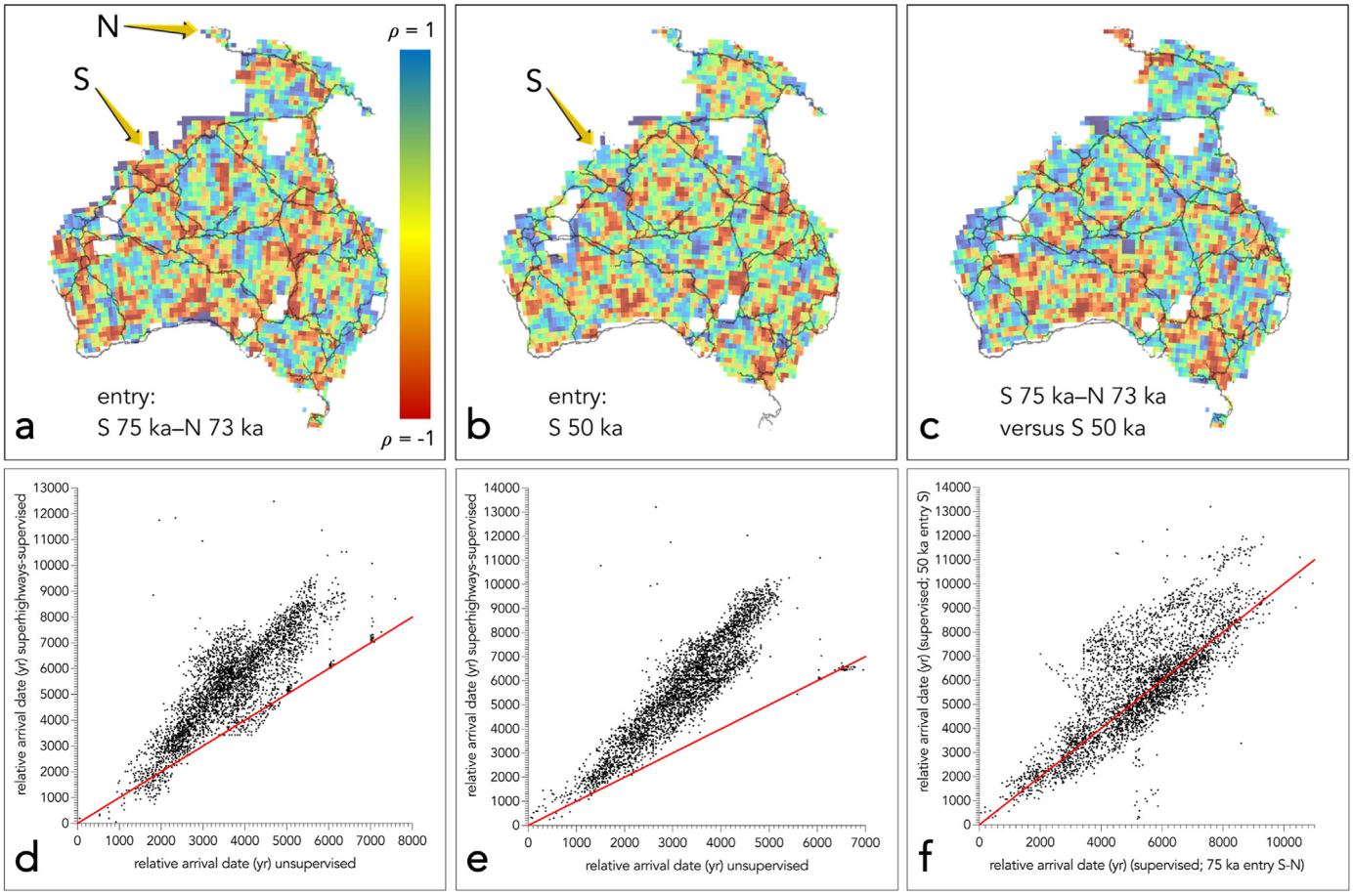

Fig. 8. Spatial correlations of arrival time. Pixel-level (0.5° × 0.5° resolution) Spearman's ρ correlation (varying from −1 to 1 following a colour scale ranging from red to blue, respectively) between (**a**) predicted initial arrival time between the unsupervised (Bradshaw et al., 2021) and superhighways-supervised models based the double-entry scenario (first at 75 ka in the south [S], followed by another at 73 ka in the north [N]) — Spearman's $\rho = 0.816$. (**b**) As in (a), but with for the single-entry scenario (50 ka in the south; $\rho = 0.903$). (**c**) Predicted initial arrival time between the two main scenarios (75 ka S–73 ka N *versus* 50 ka S) based on the superhighways-supervised models only ($\rho = 0.747$). In panels **d**–**f**, the predicted initial arrival times corresponding to panels a, b, and c, respectively are shown for each comparison, with the 1:1 line as a red line.

(southern entry) toward the Great Australian Bight. This pattern clearly differs from the single-entry scenario because a single, southern entry directs migrants first toward New Guinea along the dominant superhighways north of the Kimberley region (Figs. 2, 3 and 5), and then south-eastwards later. In contrast, the double-entry scenarios lead to rapid, early peopling of New Guinea via the delayed northern entry, such that the southern-entry populations are more quickly directed to the south and southeast via the superhighways (Figs. 2–4).

The addition of the superhighways probability layer in the model also solves the apparent anomaly associated with the late-entry (50 ka) scenarios supported in Bradshaw et al. (2021), whereby Tasmania did not become settled because by the time people reach the south-eastern extreme of Sahul, Bass Strait was flooded. In the updated model here, the slower progress across the continent means that by the time the south-eastern coast is achieved, Bass Strait is again exposed to allow people to cross into Tasmania by ~9000–10000 after initial entry. The pattern also now aligns more closely with the archaeological record in the southeast of Sahul, which was generally, with some exceptions, visited only after ~40 ka, some 10,000 years after landfall. These include the well-documented human remains (WLH3) at Lake Mungo (Bowler and Price, 1998) (~42 ka), various artefactual remains and hearths from Lake Menindee (Cupper and Duncan, 2006) (~44 ka), Dempsey Lake (Walshe, 2012) (~44 ka), and the deep alluvial deposits of the Hawkesbury-Nepean River (Cupper and Duncan, 2006; Nanson et al., 1987) ($\gtrsim$ 40 ka). In New Guinea, the data also align well with the earliest evidence of people in the Ivane Valley, probably before 43,000 years ago (Summerhayes et al., 2010). The initial peak in artefacts at Warrayti rockshelter in the Flinders Ranges also dates to ~41 ka, despite the authors suggesting an earlier initiation (Hamm et al., 2016). It is also noticeable that Warratyi, one of the earliest sites on the south coast of Sahul, is situated within the early southern-movement corridor found in the double-entry models (Hamm et al., 2016; Nanson et al., 1987; O'Connell et al., 2018). The combined model framework now also provides a more data-driven means to predict how people likely moved through, settled, and abandoned different regions in response to future periods of climatic stress (e.g., during the Last Glacial Maximum 29 ka–18 ka) (Cadd et al., 2021; Williams, 2013; Williams et al., 2013).

The maximum movement rates to continental saturation implied by the superhighways-supervised model are now approximately half (~0.4 km year^{-1}) those predicted from the unsupervised cellular automaton (Bradshaw et al., 2021) (0.7–0.9 km year^{-1}). The slower rate of progression driven by the superhighways probability layer questions faster rates suggested by previous comparisons of estimated dates among archaeological sites in Sahul (Tobler et al., 2017).

Others have suggested that human choice could have impacted dispersal spread, where topography interacting with movement decisions generally slowed dispersal (Wren, 2014). In Wren's work (Wren, 2014), a simplified landscape taking hills, gradients, and fractal landscapes into account slowed waves of advance. Several other agent-based and cellular-automaton models (Fort, 2003; Hölzchen et al., 2022; Hughes et al., 2007; Mithen and Reed, 2002; Nikitas and Nikita, 2005; Romanowska et al., 2017; Surovell, 2003; Young and Bettinger, 1995) have made assumptions about the speed of hominin dispersal using simplified topography. For example, Surovell's model (Surovell, 2003) of human spread toward Monte Verde (Chile) examined the plausibility of coastal migration *versus* inland migration. But neither scenario accounted for realistic underlying geophysical attributes of the landscape, which might slow the estimated speed of dispersal, especially for an inland route. If realistic topography slows spread in a similar fashion, we hypothesise that an Americas-specific version of the combined model might also estimate slower migration rates than what the current archaeological evidence suggests. This would potentially imply earlier dates of arrival or the dispersal in boats along a coastal route required for rapid spread to be possible. These results together suggest that underlying geomorphic attributes should be taken into account for models of dispersal, and could suggest that many estimates of time to saturation will need to be re-evaluated.

Assuming the structure of Late Pleistocene superhighways remained approximately constant up to the present is a simplification that needs to be revisited with more modern archaeological datasets. Even though the underlying viewshed structure and human physiology elements of the superhighways model are unlikely to differ markedly through time, the position of coastlines, different vegetation structures, water availability, and the presence of existing populations could potentially alter the prediction of the most ideal movement corridors (Crabtree et al., 2021). In addition, as more, reliable archaeological ages are estimated from sites across the entirety of the Sahul region, a better spatial coverage at important periods throughout the entire period of human occupancy in Sahul will hone our inferences about the patterns and timing of initial peopling.

Importantly, the models we present here demonstrate both the technological advances in combining path models and cellular automata, and that more advanced models accounting for human decision-making can more closely match the archaeological record. The ways that humans interact with terrain, ecology, and potentially other humans alter model outcomes, providing more realistic and parsimonious results. Therefore, models that incorporate only ecological and topographical features without considering the metabolic needs of travellers, as well as the opportunities and constraints to their travel, are likely to underestimate the timing of expansion into new regions. Individual decisions can lead to larger, overarching structures, even when individual agents make decisions by assessing the current conditions and addressing their movements accordingly (Crabtree et al., 2021). Stygmergic effects of a person walking on the landscape and choosing that basic path repeatedly would likely lead to migration corridors, because individuals pass on the knowledge of the landscape over time to the rest of the population. Our conclusion is therefore relevant to areas beyond Sahul; for our own models, the doubling of expansion estimates with the incorporation of the superhighway routes helped explain the expansion into south-eastern Australia, eastern New Guinea, and Tasmania. It is likely that in other regions incorporating not just demographic expansion but also traveller constraints would have important consequences for the interpretation of hominin expansion.

Our approach could be modified for other parts of the world to investigate the timing and patterns of initial peopling by anatomically modern humans, including regions of the Middle East as humans left north-eastern Africa (Groucutt et al., 2015), entry and spread into Europe (Harvati et al., 2019), expansion across southern Asia (Liu et al., 2015), and movements from Alaska to South America (Flegontov et al., 2019; Hoguin et al., 2019; Vialou et al., 2017). Coupling demographic expansion models with models of geophysical constraints and human decision-making would probably change estimates of expansion elsewhere. Because our dynamic model incorporates parameters contingent on local conditions, including the spatial patterns and magnitude of net primary production to estimate local carrying capacities, the distribution of water sources, and topographic complexity, emergent migration patterns would be highly site-specific (Dungan et al., 2018; White and Barber, 2012). In addition, both model components (cellular automaton + superhighways probability) would require independent archaeological validation for the region under

study. Similarly, including constraints such as interaction with other human/hominins would likely alter model predictions further. While Sahul was devoid of other hominins — a feature of this continent and the Americas (Esmée Webb and Rindos, 1997) — how the combination of realistic path modelling plus demographic and ecological models would impact, for example, the debates of the spread of hominins through the Horn of Africa and across Eurasia must for now remain speculative (Bergström et al., 2021; Lipson and Reich, 2017).

Combining these types of models suggest that more nuanced interpretation and scientific advancement will be considerable. While acknowledging that such complex data can result in multiple interpretations, and there will always remain a need to incorporate the broader human psyche (such as social and religious behaviour), we contend that our methods could help connect other disparate sites across the world, thereby shedding light on fundamental aspects of human migration.

Credit author statement

Corey J. A. Bradshaw: Conceptualisation, Research design, Methodology, Formal analysis, Writing – original draft, Writing – review & editing; Stephanie A. Crabtree: Conceptualisation, Writing – review & editing; Devin A. White: Conceptualisation, Writing – review & editing; Sean Ulm: Conceptualisation, Writing – review & editing; Michael I. Bird: Conceptualisation Writing – review & editing; Alan N. Williams: Conceptualisation, Writing – review & editing; Frédérik Saltré;: Conceptualisation, Writing – review & editing.

Declaration of competing interest

The authors declare that they have no known competing financial interests or personal relationships that could have appeared to influence the work reported in this paper.

All data needed to run the cellular-automaton models are available at github.com/cjabradshaw/SahulHumanSpread (https://doi.org/10.5281/zenodo.4453767). Code and relevant data for the superhighways model are available at github. com/dawhite/sfa (https://doi.org/10.5281/zenodo.7017860). All R code and data to run the hybrid superhighways–cellular-automaton model are available at github.com/cjabradshaw/SuperhighwaysSpreadModel (https://doi.org/10.5281/zenodo.7015957). Archaeological data used to validate both component models are available at github. com/cjabradshaw/SahulHumanSpread (https://doi.org/10.5281/zenodo.4453767) and static-content. springer.com/esm/art%3A10.1038%2Fs41562-021-01106-8/MediaObjects/41,562_2021_1106_MOESM3_ESM.xlsx.

Data availability

doi:10.5281/zenodo.445376; doi:10.5281/zenodo.7017860; doi:10.5281/zenodo.7015957; static-content.springer.com/esm/art%3A10.1038%2Fs41562-021-01106-8/MediaObjects/41562_2021_1106_MOESM3_ESM.xlsx

Acknowledgements

Conceptualisation: CJAB, SAC, DAW, SU, MIB, ANW, FS; Research design: CJAB; Analysis: CJAB; Writing—original draft: CJAB; Writing—review & editing: SAC, DAW, SU, MIB, ANW, FS. All authors gave final approval for publication and agreed to be held accountable for the work done therein. Funded via Australian Research Council Centre of Excellence for Australian Biodiversity and Heritage CE170100015 (SU, MIB, CJAB), Australian Research Council Future Fellowship FT120100656 (SU), and Australian Research Council Laureate Fellowship FL140100044 (MIB). Sandia National Laboratories is a multimission laboratory managed and operated by National Technology & Engineering Solutions of Sandia, LLC, a wholly owned subsidiary of Honeywell International Inc., for the U.S. Department of Energy's National Nuclear Security Administration under contract DE-NA0003525. This paper describes objective technical results and analysis. Any subjective views or opinions that might be expressed in the paper do not necessarily represent the views of the U.S. Department of Energy or the United States Government.

References

Allen, J.I.M., O'Connell, J.F., 2020. A different paradigm for the initial colonisation of Sahul. Archaeol. Ocean. 55, 1–14.
Baddeley, A., Rubak, E., Turner, R., 2015. Spatial Point Patterns: Methodology and Applications with R. Chapman and Hall/CRC Press, Boca Raton, Florida.
Bergström, A., Nagle, N., Chen, Y., McCarthy, S., Pollard, Martin O., Ayub, Q., Wilcox, S., Wilcox, L., van Oorschot, Roland, A.H., McAllister, P., Williams, L., Xue, Y., Mitchell, R.J., Tyler-Smith, C., 2016. Deep roots for Aboriginal Australian Y chromosomes. Curr. Biol. 26, 809–813.
Bergström, A., Stringer, C., Hajdinjak, M., Scerri, E.M.L., Skoglund, P., 2021. Origins of modern human ancestry. Nature 590, 229–237.
Binford, L.R., 2001. Constructing Frames of Reference: an Analytical Method for Archaeological Theory Building Using Ethnographic and Environmental Data Sets. University of California Press, Berkeley.
Bird, M.I., Beaman, R.J., Condie, S.A., Cooper, A., Ulm, S., Veth, P., 2018. Palaeogeography and voyage modeling indicates early human colonization of Australia was likely from Timor-Roti. Quat. Sci. Rev. 191, 431–439.
Bird, M.I., Condie, S.A., O'Connor, S., O'Grady, D., Reepmeyer, C., Ulm, S., Zega, M., Saltré, F., Bradshaw, C.J.A., 2019. Early human settlement of Sahul was not an accident. Sci. Rep. 9, 8220.
Bird, M.I., O'Grady, D., Ulm, S., 2016. Humans, water, and the colonization of Australia. Proc. Natl. Acad. Sci. U.S.A. 113, 11477–11482.
Bowler, J.M., Price, D.M., 1998. Luminescence dates and stratigraphic analyses at Lake Mungo: review and new perspectives. Archaeol. Ocean. 33, 156–168.
Bradshaw, C.J.A., Norman, K., Ulm, S., Williams, A.N., Clarkson, C., Chadoeuf, J., Lin, S.C., Jacobs, Z., Roberts, R.G., Bird, M.I., Weyrich, L.S., Haberle, S.G., O'Connor, S., Llamas, B., Cohen, T.J., Friedrich, T., Veth, P., Leavesley, M., Saltré, F., 2021. Stochastic models support rapid peopling of Late Pleistocene Sahul. Nat. Commun. 12, 2440.
Bradshaw, C.J.A., Ulm, S., Williams, A.N., Bird, M.I., Roberts, R.G., Jacobs, Z., Laviano, F., Weyrich, L.S., Friedrich, T., Norman, K., Saltré, F., 2019. Minimum founding populations for the first peopling of Sahul. Nat. Ecol. Evol. 3, 1057–1063.
Bulbeck, D., 2007. Where river meets sea: a parsimonious model for *Homo sapiens* colonization of the Indian Ocean Rim and Sahul. Curr. Anthropol. 48, 315–321.
Cadd, H., Petherick, L., Tyler, J., Herbert, A., Cohen, T.J., Sniderman, K., Barrows, T.T., Fulop, R.H., Knight, J., Kershaw, A.P., Colhoun, E.A., Harris, M.R.P., 2021. A continental perspective on the timing of environmental change during the last glacial stage in Australia. Quat. Res. 102, 5–23.
Chamberlain, A., 2009. Archaeological demography. Hum. Biol. 81, 275–287.
Clarkson, C., Jacobs, Z., Marwick, B., Fullagar, R., Wallis, L., Smith, M., Roberts, R.G., Hayes, E., Lowe, K., Carah, X., Florin, S.A., McNeil, J., Cox, D., Arnold, L.J., Hua, Q., Huntley, J., Brand, H.E.A., Manne, T., Fairbairn, A., Shulmeister, J., Lyle, L., Salinas, M., Page, M., Connell, K., Park, G., Norman, K., Murphy, T., Pardoe, C., 2017. Human occupation of northern Australia by 65,000 years ago. Nature 547, 306–310.
Crabtree, S.A., White, D.A., Bradshaw, C.J.A., Saltré, F., Williams, A.N., Beaman, R.J., Bird, M.I., Ulm, S., 2021. Landscape rules predict optimal super-highways for the first peopling of Sahul. Nat. Human Behav. 5, 1303–1313.
Cupper, M.L., Duncan, J., 2006. Last glacial megafaunal death assemblage and early human occupation at Lake Menindee, southeastern Australia. Quat. Res. 66, 332–341.
Dortch, J., Malaspinas, A.-S., 2017. Madjedbebe and genomic histories of Aboriginal Australia. Aust. Archaeol. 83, 174–177.
Dungan, K.A., White, D., Déderix, S., Mills, B.J., Safi, K., 2018. A total viewshed approach to local visibility in the Chaco World. Antiquity 92, 905–921.
Esmée Webb, R., Rindos, D.J., 1997. The mode and tempo of the initial human colonisation of empty landmasses: Sahul and the Americas compared. Archaeol. Pap. Am. Anthropol. Assoc. 7, 233–250.
Flegontov, P., Altınışık, N.E., Changmai, P., Rohland, N., Mallick, S., Adamski, N., Bolnick, D.A., Broomandkhoshbacht, N., Candilio, F., Culleton, B.J., Flegontova, O., Friesen, T.M., Jeong, C., Harper, T.K., Keating, D., Kennett, D.J., Kim, A.M., Lamnidis, T.C., Lawson, A.M., Olalde, I., Oppenheimer, J., Potter, B.A., Raff, J., Sattler, R.A., Skoglund, P., Stewardson, K., Vajda, E.J., Vasilyev, S., Veselovskaya, E., Hayes, M.G., O'Rourke, D.H., Krause, J., Pinhasi, R., Reich, D., Schiffels, S., 2019. Palaeo-Eskimo genetic ancestry and the peopling of Chukotka and North America. Nature 570, 236–240.

Fort, J., 2003. Population expansion in the western Pacific (Austronesia): a wave of advance model. Antiquity 77, 520–530.
Frachetti, M.D., Smith, C.E., Traub, C.M., Williams, T., 2017. Nomadic ecology shaped the highland geography of Asia's Silk Roads. Nature 543, 193–198.
Frankenfield, D., Roth-Yousey, L., Compher, C., 2005. Comparison of predictive equations for resting metabolic rate in healthy nonobese and obese adults: a systematic review. J. Am. Diet Assoc. 105, 775–789.
Goosse, H., Brovkin, V., Fichefet, T., Haarsma, R., Mouchet, A., Selten, F., Barriat, P.-Y., Campin, J.-M., Deleersnijder, E., Driesschaert, E., Goelzer, H., Janssens, I., Loutre, M.-F., Morales Maqueda, M.A., Opsteegh, T., Mathieu, P.-P., Munhoven, G., Pettersson, E.J., Renssen, H., Roche, D.M., Schaeffer, M., Tartinville, B., Timmermann, A., Weber, S.L., P., H., J., J., 2010. Description of the Earth system model of intermediate complexity LOVECLIM version 1.2. Geosci. Model Dev. 3, 603–633.
Groucutt, H.S., Petraglia, M.D., Bailey, G., Scerri, E.M.L., Parton, A., Clark-Balzan, L., Jennings, R.P., Lewis, L., Blinkhorn, J., Drake, N.A., Breeze, P.S., Inglis, R.H., Devès, M.H., Meredith-Williams, M., Boivin, N., Thomas, M.G., Scally, A., 2015. Rethinking the dispersal of *Homo sapiens* out of Africa. Evol. Anthropol. Issues News Rev. 24, 149–164.
Hamm, G., Mitchell, P., Arnold, L.J., Prideaux, G.J., Questiaux, D., Spooner, N.A., Levchenko, V.A., Foley, E.C., Worthy, T.H., Stephenson, B., Coulthard, V., Coulthard, C., Wilton, S., Johnston, D., 2016. Cultural innovation and megafauna interaction in the early settlement of arid Australia. Nature 539, 280–283.
Harvati, K., Röding, C., Bosman, A.M., Karakostis, F.A., Grün, R., Stringer, C., Karkanas, P., Thompson, N.C., Koutoulidis, V., Moulopoulos, L.A., Gorgoulis, V.G., Kouloukoussa, M., 2019. Apidima Cave fossils provide earliest evidence of *Homo sapiens* in Eurasia. Nature 571, 500–504.
Hiscock, P., 2008. Archaeology of Ancient Australia. Routledge, London.
Hiscock, P., 2017. Discovery curves, colonisation and Madjedbebe. Aust. Archaeol. 83, 168–171.
Hoguin, R., Franco, N.V., Flegenheimer, N., 2019. Humans, technology, and environment in the early peopling of South America. PaleoAmerica 5, 307–308.
Hölzchen, E., Hertler, C., Willmes, C., Anwar, I.P., Mateos, A., Rodríguez, J., Berndt, J.O., Timm, I.J., 2022. Estimating crossing success of human agents across sea straits out of Africa in the Late Pleistocene. Paleogeogr. Paleoclimatol. Paleoecol. 590, 110845.
Hughes, J.K., Haywood, A., Mithen, S.J., Sellwood, B.W., Valdes, P.J., 2007. Investigating early hominin dispersal patterns: developing a framework for climate data integration. J. Hum. Evol. 53, 465–474.
Kealy, S., Louys, J., O'Connor, S., 2018. Least-cost pathway models indicate northern human dispersal from Sunda to Sahul. J. Hum. Evol. 125, 59–70.
Kiskowski, M.A., Hancock, J.F., Kenworthy, A.K., 2009. On the use of Ripley's *K*-function and its derivatives to analyze domain size. Biophys. J. 97, 1095–1103.
Lipson, M., Reich, D., 2017. A working model of the deep relationships of diverse modern human genetic lineages outside of Africa. Mol. Biol. Evol. 34, 889–902.
Liu, W., Martinón-Torres, M., Cai, Y.-j., Xing, S., Tong, H.-w., Pei, S.-w., Sier, M.J., Wu, X.-h., Edwards, R.L., Cheng, H., Li, Y.-y., Yang, X.-x., de Castro, J.M.B., Wu, X.-j., 2015. The earliest unequivocally modern humans in southern China. Nature 526, 696–699.
Lorenz, D.J., Nieto-Lugilde, D., Blois, J.L., Fitzpatrick, M.C., Williams, J.W., 2016. Downscaled and debiased climate simulations for North America from 21,000 years ago to 2100 AD. Sci. Data 3, 160048.
Malaspinas, A.-S., Westaway, M.C., Muller, C., Sousa, V.C., Lao, O., Alves, I., Bergström, A., Athanasiadis, G., Cheng, J.Y., Crawford, J.E., Heupink, T.H., Macholdt, E., Peischl, S., Rasmussen, S., Schiffels, S., Subramanian, S., Wright, J.L., Albrechtsen, A., Barbieri, C., Dupanloup, I., Eriksson, A., Margaryan, A., Moltke, I., Pugach, I., Korneliussen, T.S., Levkivskyi, I.P., Moreno-Mayar, J.V., Ni, S., Racimo, F., Sikora, M., Xue, Y., Aghakhanian, F.A., Brucato, N., Brunak, S., Campos, P.F., Clark, W., Ellingvåg, S., Fourmile, G., Gerbault, P., Injie, D., Koki, G., Leavesley, M., Logan, B., Lynch, A., Matisoo-Smith, E.A., McAllister, P.J., Mentzer, A.J., Metspalu, M., Migliano, A.B., Murgha, L., Phipps, M.E., Pomat, W., Reynolds, D., Ricaut, F.-X., Siba, P., Thomas, M.G., Wales, T., Wall, C.M.r., Oppenheimer, S.J., Tyler-Smith, C., Durbin, R., Dortch, J., Manica, A., Schierup, M.H., Foley, R.A., Lahr, M.M., Bowern, C., Wall, J.D., Mailund, T., Stoneking, M., Nielsen, R., Sandhu, M.S., Excoffier, L., Lambert, D.M., Willerslev, E., 2016. A genomic history of Aboriginal Australia. Nature 538, 207–214.
McNiven, I.J., 1999. Fissioning and regionalisation: the social dimensions of changes in Aboriginal use of the Great Sandy Region, southeast Queensland. In: Hall, H.J., McNiven, I.J. (Eds.), Australian Coastal Archaeology. ANH Publications, Australian National University, Department of Archaeology and Natural History, Canberra, pp. 157–168.
Mifflin, M.D., St Jeor, S.T., Hill, L.A., Scott, B.J., Daugherty, S.A., Koh, Y.O., 1990. A new predictive equation for resting energy expenditure in healthy individuals. Am. J. Clin. Nutr. 51, 241–247.
Mithen, S., Reed, M., 2002. Stepping out: a computer simulation of hominid dispersal from Africa. J. Hum. Evol. 43, 433–462.
Nagle, N., Ballantyne, K.N., van Oven, M., Tyler-Smith, C., Xue, Y., Wilcox, S., Wilcox, L., Turkalov, R., van Oorschot, R.A.H., van Holst Pellekaan, S., Schurr, T.G., McAllister, P., Williams, L., Kayser, M., Mitchell, R.J., The Genographic, C., Adhikarla, S., Adler, C.J., Balanovska, E., Balanovsky, O., Bertranpetit, J., Clarke, A.C., Comas, D., Cooper, A., Der Sarkissian, C.S.I., Dulik, M.C., Gaieski, J.B., GaneshPrasad, A., Haak, W., Haber, M., Hobbs, A., Javed, A., Jin, L., Kaplan, M.E., Li, S., Martínez-Cruz, B., Matisoo-Smith, E.A., Melé, M., Merchant, N.C., Owings, A.C., Parida, L., Pitchappan, R., Platt, D.E., Quintana-Murci, L., Renfrew, C., Royyuru, A.K., Santhakumari, A.V., Santos, F.R., Soodyall, H., Hernanz, D.F.S., Swamikrishnan, P., Vilar, M.G., Wells, R.S., Zalloua, P.A., Ziegle, J.S., 2017. Mitochondrial DNA diversity of present-day Aboriginal Australians and implications for human evolution in Oceania. J. Hum. Genet. 62, 343–353.
Nanson, G.C., Young, R.W., Stockton, E.D., 1987. Chronology and palaeoenvironment of the Cranebrook Terrace (near Sydney) containing artefacts more than 40,000 years old. Archaeol. Ocean. 22, 72–78.
Nikitas, P., Nikita, E., 2005. A study of hominin dispersal out of Africa using computer simulations. J. Hum. Evol. 49, 602–617.
Norman, K., Inglis, J., Clarkson, C., Faith, J.T., Shulmeister, J., Harris, D., 2018. An early colonisation pathway into northwest Australia 70-60,000 years ago. Quat. Sci. Rev. 180, 229–239.
O'Connell, J.F., Allen, J., 2012. The restaurant at the end of the universe: modelling the colonisation of Sahul. Aust. Archaeol. 74, 5–17.
O'Connell, J.F., Allen, J., Williams, M.A.J., Williams, A.N., Turney, C.S.M., Spooner, N.A., Kamminga, J., Brown, G., Cooper, A., 2018. When did *Homo sapiens* first reach Southeast Asia and Sahul? Proc. Natl. Acad. Sci. U.S.A. 115, 8482–8490.
Pandolf, K.B., Givoni, B., Goldman, R.F., 1977. Predicting energy expenditure with loads while standing or walking very slowly. J. Appl. Physiol. 43, 577–581.
Pedro, N., Brucato, N., Fernandes, V., André, M., Saag, L., Pomat, W., Besse, C., Boland, A., Deleuze, J.-F., Clarkson, C., Sudoyo, H., Metspalu, M., Stoneking, M., Cox, M.P., Leavesley, M., Pereira, L., Ricaut, F.-X., 2020. Papuan mitochondrial genomes and the settlement of Sahul. J. Hum. Genet. 65, 875–887.
Roberts-Thomson, J.M., Martinson, J.J., Norwich, J.T., Harding, R.M., Clegg, J.B., Boettcher, B., 1996. An ancient common origin of aboriginal Australians and New Guinea highlanders is supported by alpha-globin haplotype analysis. Am. J. Hum. Genet. 58, 1017–1024.
Romanowska, I., Gamble, C., Bullock, S., Sturt, F., 2017. Dispersal and the Movius Line: testing the effect of dispersal on population density through simulation. Quat. Int. 431, 53–63.
Saltré, F., Chadoeuf, J., Peters, K.J., McDowell, M.C., Friedrich, T., Timmermann, A., Ulm, S., Bradshaw, C.J.A., 2019. Climate-human interaction associated with southeast Australian megafauna extinction patterns. Nat. Commun. 10, 5311.
Saltré, F., Chuine, I., Brewer, S., Gaucherel, C., 2009. A phenomenological model without dispersal kernel to model species migration. Ecol. Model. 220, 3546–3554.
Santee, W., Blanchard, L., Speckman, K., Gonzales, J., Wallace, R., 2003. Load Carriage Model Development and Testing with Field Data. United States Army Research Institute of Environmental Medicine, Natick, MA.
Summerhayes, G.R., Leavesley, M., Fairbairn, A., Mandui, H., Field, J., Ford, A., Fullagar, R., 2010. Human adaptation and plant use in Highland New Guinea 49,000 to 44,000 years ago. Science 330, 78–81.
Surovell, T.A., 2003. Simulating coastal migration in New World colonization. Curr. Anthropol. 44, 580–591.
Tallavaara, M., Eronen, J.T., Luoto, M., 2018. Productivity, biodiversity, and pathogens influence the global hunter-gatherer population density. Proc. Natl. Acad. Sci. U.S.A. 115, 1232–1237.
Timmermann, A., Friedrich, T., 2016. Late Pleistocene climate drivers of early human migration. Nature 538, 92–95.
Tobler, R., Rohrlach, A., Soubrier, J., Bover, P., Llamas, B., Tuke, J., Bean, N., Abdullah-Highfold, A., Agius, S., O'Donoghue, A., O'Loughlin, I., Sutton, P., Zilio, F., Walshe, K., Williams, A.N., Turney, C.S.M., Williams, M., Richards, S.M., Mitchell, R.J., Kowal, E., Stephen, J.R., Williams, L., Haak, W., Cooper, A., 2017. Aboriginal mitogenomes reveal 50,000 years of regionalism in Australia. Nature 544, 180–184.
Tobler, W., 1993. Three Presentations on Geographial Analysis and Modeling. National Center for Geographic Information and Analysis, Buffalo, NY.
Vahdati, A.R., Weissmann, J.D., Timmermann, A., Ponce de León, M.S., Zollikofer, C.P.E., 2019. Drivers of Late Pleistocene human survival and dispersal: an agent-based modeling and machine learning approach. Quat. Sci. Rev. 221, 105867.
Veth, P., 2017. Breaking through the radiocarbon barrier: Madjedbebe and the new chronology for Aboriginal occupation of Australia. Aust. Archaeol. 83, 165–167.
Vialou, D., Benabdelhadi, M., Feathers, J., Fontugne, M., Vialou, A.V., 2017. Peopling South America's centre: the late Pleistocene site of Santa Elina. Antiquity 91, 865–884.
Walshe, K., 2012. Port Augusta hearth site dated to 40,000 years. Aust. Archaeol. 74, 106–110.
White, D.A., Barber, S.B., 2012. Geospatial modeling of pedestrian transportation networks: a case study from precolumbian Oaxaca, Mexico. J. Archaeol. Sci. 39, 2684–2696.
Wilby, R.L., Wigley, T.M.L., 1997. Downscaling general circulation model output: a review of methods and limitations. Prog. Phys. Geogr. Earth Environ. 21, 530–548.
Williams, A.N., 2013. A new population curve for prehistoric Australia. Proc. Roy. Soc. Lond. B 280, 20130486.
Williams, A.N., Ulm, S., Cook, A.R., Langley, M.C., Collard, M., 2013. Human refugia in Australia during the Last Glacial Maximum and Terminal Pleistocene: a geospatial analysis of the 25–12 ka Australian archaeological record. J. Archaeol. Sci. 40, 4612–4625.

Wood, R., 2017. Comments on the chronology of Madjedbebe. Aust. Archaeol. 83, 172–174.
Wren, C., 2014. The Effect of Spatial Environment Heterogeneity on Hominin Dispersal Events and the Evolution of Complex Cognition. Department of Anthropology, Montréal McGill University. PhD thesis.
Young, D.A., Bettinger, R.L., 1995. Simulating the global human expansion in the Late Pleistocene. J. Archaeol. Sci. 22, 89–92.
Yuen, L.K.W., Littlejohn, M., Duchêne, S., Edwards, R., Bukulatjpi, S., Binks, P., Jackson, K., Davies, J., Davis, J.S., Tong, S.Y.C., Locarnini, S., 2019. Tracing ancient human migrations into Sahul using hepatitis B virus genomes. Mol. Biol. Evol. 36, 942–954.